



HAL
open science

Mechanistic insights into β -oxygen atom transfer in olefinepoxidation mediated by W(vi) complexes and H₂O₂

Chiara Dinoi, Rinaldo Poli, Lionel Perrin, Laurent Maron

► **To cite this version:**

Chiara Dinoi, Rinaldo Poli, Lionel Perrin, Laurent Maron. Mechanistic insights into β -oxygen atom transfer in olefinepoxidation mediated by W(vi) complexes and H₂O₂. Dalton Transactions, 2012, 41 (4), pp.1131-1133. 10.1039/c1dt10924c . hal-02909748

HAL Id: hal-02909748

<https://hal.science/hal-02909748>

Submitted on 2 Mar 2021

HAL is a multi-disciplinary open access archive for the deposit and dissemination of scientific research documents, whether they are published or not. The documents may come from teaching and research institutions in France or abroad, or from public or private research centers.

L'archive ouverte pluridisciplinaire **HAL**, est destinée au dépôt et à la diffusion de documents scientifiques de niveau recherche, publiés ou non, émanant des établissements d'enseignement et de recherche français ou étrangers, des laboratoires publics ou privés.

Mechanistic insights into β -oxygen atom transfer in olefin epoxidation mediated by W(VI) complexes and H_2O_2

Chiara Dinoi,^{a,b} Rinaldo Poli,^{b,c} Lionel Perrin^{*a} and Laurent Maron^{*a,c}

Received (in XXX, XXX) Xth XXXXXXXXX 200X, Accepted Xth XXXXXXXXX 200X

5 First published on the web Xth XXXXXXXXX 200X

DOI: 10.1039/b000000x

A DFT investigation of the olefin epoxidation mechanism catalysed by the $[\text{Cp}^*\text{WO}(\text{OH})_2]^+$ complex with H_2O_2 reveals that the outer sphere transfer of the hydroperoxido O^β atom to the olefin is considerably more favourable than that of the hydroperoxido O^α atom. The reasons for this unusual pathway are discussed.

Alkene epoxidation is one of the fundamental and straightforward reactions in functionalising hydrocarbons as well as rapidly building selective functionality into a wide range of molecules.^{1,2} High scale production of epoxides needs the development of new synthetic methods that employ safe oxidants and produce as little waste as possible. In that perspective, hydrogen peroxide is an attractive oxygen source, both on environmental and economic grounds.^{3,4} It is cheap, readily available and gives water as the only by-product. Among the different transition metal catalysts used to carry out this transformation, high oxidation state cyclopentadienyl Mo- and W-oxido compounds have attracted great attention due to their rich aqueous chemistry⁵⁻⁷ as well as to their ability to catalyse the olefin epoxidation in the presence of H_2O_2 in both organic and aqueous media.⁸⁻¹⁰

As previously reported by our groups, in particular, the $\text{Cp}^*\text{W}_2\text{O}_5$ complex efficiently catalyzes the cyclooctene (COE) epoxidation with aqueous H_2O_2 in acetonitrile/toluene, showing a much greater catalytic activity than its corresponding Mo analogue.^{9,10} Computational studies, in addition, have recently unveiled the olefin epoxidation mechanism catalysed by the $\text{Cp}^*\text{MO}_2\text{Cl}$ ($\text{M} = \text{Mo}, ^{8-10} \text{W}^{9,10}$) and $[\text{Cp}^*\text{MO}_2(\text{H}_2\text{O})]^+$ ($\text{M} = \text{Mo}^8$) complexes as models for the catalysts in organic and aqueous solvents respectively. On the basis of these results, we decided to theoretically investigate the $\text{Cp}^*\text{W}^{\text{VI}}$ -catalysed olefin epoxidation reaction by H_2O_2 in the presence of water. By extension of the speciation of $\text{Cp}^*\text{W}_2\text{O}_5$ to the W analogue in aqueous media,⁵⁻⁷ $\text{Cp}^*\text{W}_2\text{O}_5$ should also act as an electrolyte in water, producing the $[\text{Cp}^*\text{WO}_2(\text{H}_2\text{O})]^+$ or the tautomeric $[\text{Cp}^*\text{WO}(\text{OH})_2]^+$ cation as the catalytic active species. The formation of these species as the major compound in aqueous solution has been proven by an ESI-MS experiment. As shown in the ESI Fig S1, the strongest peak of the positive-mode ESI-MS spectrum of a 0.1 mM MeOH- H_2O (1:1) solution of $\text{Cp}^*\text{W}_2\text{O}_5$ corresponds to the water addition product $[\text{Cp}^*\text{WO}_2(\text{H}_2\text{O})]^+$ peak ($m/z = 367-372$) (or to the tautomeric dihydroxido species $[\text{Cp}^*\text{WO}(\text{OH})_2]^+$). By geometry optimisation in gas phase and in water, $[\text{Cp}^*\text{WO}(\text{OH})_2]^+$ resulted more stable than the corresponding water adduct by

21.4 and 13.1 kcal mol⁻¹, respectively. Here, hence, we report a theoretical study¹¹ on the olefin epoxidation mechanism using the $[\text{Cp}^*\text{WO}(\text{OH})_2]^+$ complex as a model for the active catalyst in water. In view of the recent progress related to oxotransferase tungsten-containing enzymes,¹²⁻¹⁴ in particular, our goal is to gain further insight into the comprehension of the oxygen transfer epoxidation process involving the WO_2 fragment and especially into the relation between the electronic structure of the catalyst and the oxygen transfer pathways involved during the catalytic cycle in aqueous media.

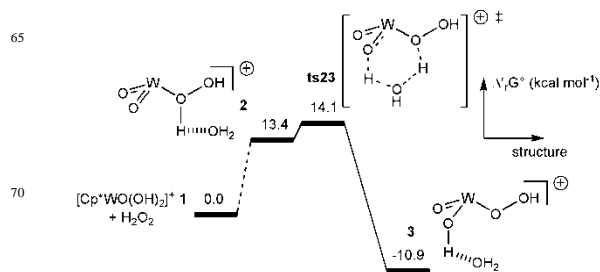
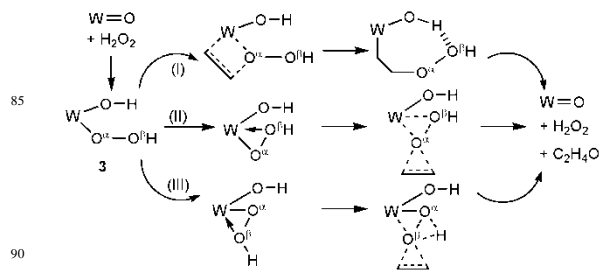


Fig. 1 Free enthalpy profile (kcal mol⁻¹) for the H_2O_2 activation by $[\text{Cp}^*\text{WO}(\text{OH})_2]^+$. Cp^* omitted for clarity.

Taking complex $[\text{Cp}^*\text{WO}(\text{OH})_2]^+$ (**1**) as the starting point, the first step of the catalytic pathway involves the H_2O_2 activation (Fig 1). Thermodynamically, the reaction is exoergonic by 10.9 kcal mol⁻¹ and proceeds with an energy barrier of 14.1 kcal mol⁻¹ with respect to the separated reactants.



Scheme 1. Cp^* omitted for clarity.

The reaction continues with the approach of the olefin followed by the oxygen transfer from the activated oxidant to the incoming olefin. Starting from **3**, three possible pathways can occur (scheme 1): I) insertion of the olefin in to the W-OOH bond (called hereafter the Mimoun¹⁵ pathway); II) external O^α atom transfer to the olefin and III) external O^β

atom transfer to the olefin accompanied by a proton transfer from O^β to O^α (Scheme 1).

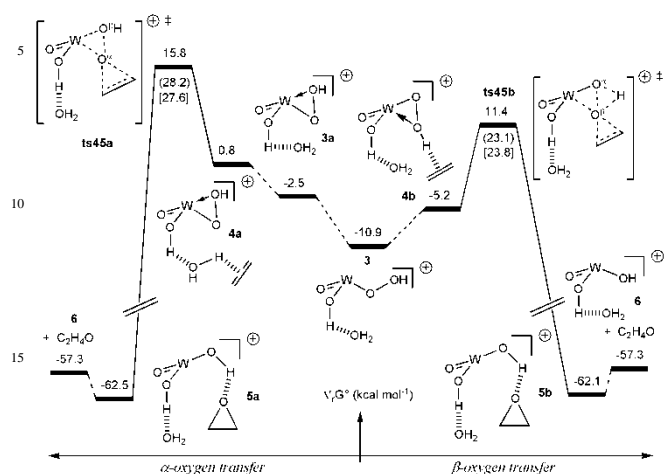


Fig. 2 Free enthalpy profile (kcal mol⁻¹) for the oxygen atom transfer from **3** to ethylene. Cp* omitted for clarity.

The calculated Mimoun profile leads to prohibitive activation energies and will not be further discussed here. Concerning the external pathway, both mechanisms II) and III) have been computed (Fig. 2). Both pathways are exoergonic and lead, through transition states **ts45a** and **ts45b** (respectively 26.6 and 22.2 kcal mol⁻¹ relative to **3**), to [Cp*WO(OH)₂]⁺·H₂O (**6**) and C₂H₄O. Optimised geometries of the transition states are shown in the ESI, Fig.S2.

Interestingly, the energy barrier corresponding to the O^α transfer (**ts45a**) is ca. 5 kcal mol⁻¹ higher than that of O^β (**ts45b**), indicating that the latter mechanism is the most favourable pathway in the case of [Cp*WO(OH)₂]⁺.

In order to assess solvation effects, we have computed the profile reported in Fig. 2 in water and CH₃CN (ESI, Fig S3) using implicit solvent model. At this level of modeling, transition states **ts45a** and **ts45b** define energy barriers relative to **1** of 28.2 and 23.1 kcal mol⁻¹ in water and of 27.6 and 22.8 kcal mol⁻¹ in CH₃CN. These values are respectively reported in Fig. 2 in parenthesis and brackets. Though the energy barriers are modified, the trend between α - versus β -oxygen transfer remains unchanged.

The W complex, therefore, differs from the analogue Mo complex, for which the computed activation barriers of these two pathways were close in energy.⁸ It also differs from other previously reported hydroperoxido derivatives of Ti, Re, and Mo.¹⁶ The DFT studies carried out on Ti(OH)₃(OOH),¹⁷ Re(CH₃)(O₂)₂O(H₂O)¹⁸ and Mo(NH₃)(O₂)O(OH)(OOH),¹⁹ in fact, revealed the kinetic preference for the attack of the O^α of the hydroperoxido group over the attack of the O^β .

To better understand the reason of this difference and to investigate the influence of the metal electron density on the oxygen transfer mechanism, the two energy profiles (II and III) have also been recomputed for the neutral Cp*WO₂Cl complex at the same level of theory (ESI, FigS3 and Fig.3). Also for the latter system, both pathways are exoergonic, with activation barriers of 36.6 (**ts45c**) and 45.5 kcal mol⁻¹ (**ts45d**)

relative to **1**_Cl (for the geometries of the transition states see the ESI, Fig S4).

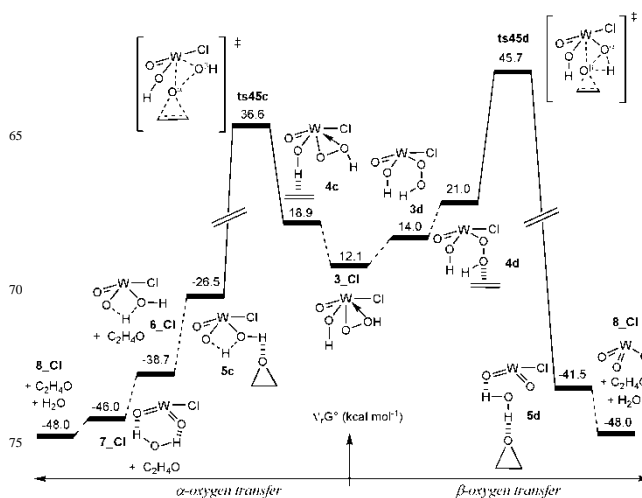


Fig. 3 Free enthalpy profile (kcal mol⁻¹) for the oxygen atom transfer from **3**_Cl to ethylene. Cp* omitted for clarity.

Differently from the cationic system **1**, however, the external attack to the O^α center (**ts45c**) is ca. 9 kcal mol⁻¹ more favourable than that to the O^β atom (**ts45d**), indicating that, within a series of similar complexes containing the same metal, the electron density at the metal center plays an important role on the operative oxygen transfer mechanism.

The Cp*WO₂Cl compound is a 16 electrons system while the corresponding [Cp*WO₂]⁺ ion is a 14 electrons system. Due to its lower electron density, the cationic [Cp*WO(OH)(OOH)]⁺·H₂O (**3**) complex is likely to form a stronger W-OOH bond compared to the neutral Cp*WOCi(OH)(OOH) complex (**3**_Cl), leading to an increase of the O^α transfer energy barrier.

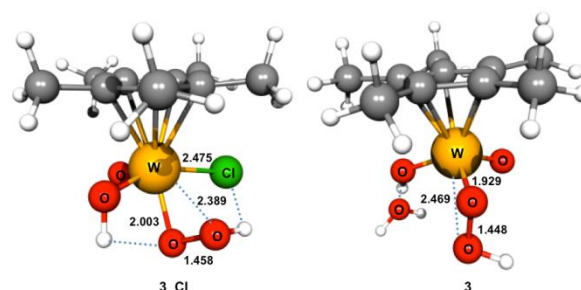


Fig. 4 Optimised geometries for the **3**_Cl and **3** systems.

In order to quantify the W- O^α bond strength, we analysed the W- O^α bond length in both neutral [Cp*WO(OH)(OOH)Cl] and cationic [Cp*WO(OH)(OOH)]⁺·H₂O systems (**3**_Cl and **3**). As shown in Figure 4, this bond is shorter in **3** than in **3**_Cl, suggesting that the direct contribution of the W- O^α bond strength to the oxygen transfer activation barrier plays an important role in pathway II.

To gain further insight into the W- O^α - O^β H and WO $^\alpha$ - O^β H bond energies for both **3**_Cl and **3**, we computed their homolytic bond dissociation energy (BDE). For the neutral complex, the energies of the W- O^α - O^β H and WO $^\alpha$ - O^β H bonds

were computed as 19.8 (W-O^α) and 22.5 (O^α-O^β) kcal mol⁻¹ respectively. For the cationic complex, on the other hand, they were computed as 51.8 (W-O^α) and 14.7 (O^α-O^β) kcal mol⁻¹, respectively, indicating that the W-O^αO^βH bond cleavage is considerably more energy demanding for the cationic than for the neutral system. In the case of the [Cp*WO(OH)(OOH)]⁺·H₂O 14 e⁻ system (**3**), therefore, the lower metal electron density results in a stronger interaction between the W center and the O^α, directing the mechanism toward the transfer of the O^β.

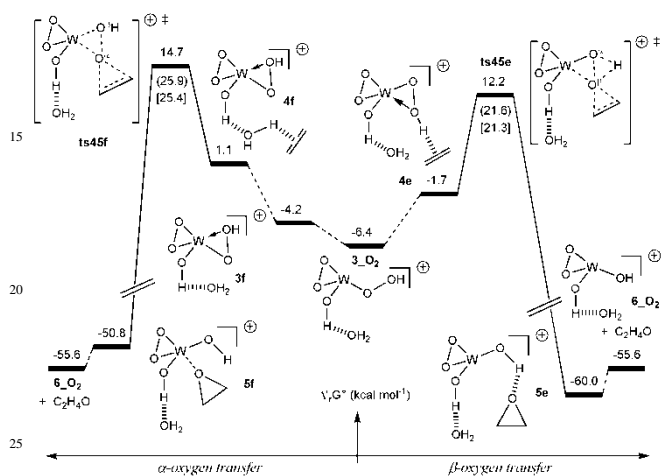


Fig. 5 Free enthalpy profile (kcal mol⁻¹) for the oxygen atom transfer from **3**_{O₂} to ethylene. Cp* omitted for clarity.

In order to validate this idea, we computed the olefin epoxidation mechanism catalysed by the cationic [Cp*W(O₂)(OH)₂]⁺ peroxido complex (more stable than the corresponding water adduct by 8.5 and 2.4 kcal mol⁻¹, in gas phase and in water respectively). (Fig. 5 and Fig. S5 in the ESI). Here again, both pathways are exoergonic and lead, through transition states **ts45e** and **ts45f** (respectively 18.5 and 21.1 kcal mol⁻¹ relative to **3**_{O₂}) to [Cp*W(O₂)(OH)₂]⁺·H₂O (**6**_{O₂}) and C₂H₄O (for the geometries of the transition states see the ESI, Fig S6). The most favourable pathway corresponds to the O^β attack (**ts45e**), the activation barrier related to the O^α transfer (**ts45f**) being ca. 3 kcal mol⁻¹ higher. The profile in shown in Fig. 5 was also computed in water and CH₃CN (ESI Fig. S8). Energy barriers associated to **ts45e** and **ts45f** are of 21.5 and 25.9 kcal mol⁻¹ in water and 21.3 and 25.4 kcal mol⁻¹ in CH₃CN relatively to **1**_{O₂}. These values are respectively reported in Fig. 5 in parenthesis and in brackets. Once again, the trend between α- versus β-oxygen transfer remaining unchanged.

According to the O^β transfer, in addition, the computed W-O^αO^βH and WO^α-O^βH homolytic bond dissociation energy (BDE) were 46.9 and 7.6 kcal mol⁻¹, respectively, indicating, once again, that the high energy of the W-O^αO^βH bond cleavage drives the system toward the O^β atom transfer.

55 Conclusions

Through a DFT study, we have investigated the olefin epoxidation mechanism catalysed by the [Cp*WO(OH)₂]⁺ and [Cp*W(O₂)(OH)₂]⁺ complexes with H₂O₂. Inspection of the

different transition states reveals that the transfer of the hydroperoxido O^β to the olefin is considerably more favourable than that of the hydroperoxido O^α. This O^β atom transfer pathway has not been previously considered as a competitive epoxidation mechanism to the best of our knowledge and has been rationalized here on the basis of the metal electron density as well as of the W-O^αO^βH and WO^α-O^βH bond energies. The stronger the interaction between the W center and the O^α, the more favourable the O^β transfer process. With the present work, we have therefore shown that within a series of similar complexes containing the same W^{VI} metal, the oxygen transfer pathway depends on the metal charge and electron density, providing further insights into the comprehension of the oxygen transfer process for the design of efficient olefin epoxidation W catalysts.

The authors thank the Institut Universitaire de France and CALMIP, CINES for grants of computing time.

Notes and references

- ^a Laboratoire de Physique et Chimie des Nano-objets (LPCNO), UMR 5215, Université de Toulouse-CNRS, INSA, UPS, 135 Avenue de Rangueil, 31077 Toulouse Cedex 4, France. Fax. 33 561 559 697; Tel. 33 561 559 664; E-mail: lionel.perrin@insa-toulouse.fr
^b CNRS; LCC (Laboratoire de Chimie de Coordination); Université de Toulouse; UPS, INPT; 205, Route de Narbonne, F-31077 Toulouse.
^c Institut Universitaire de France, 103, bd Saint-Michel, 75005 Paris, France.

† Electronic Supplementary Information (ESI) available: additional figures and cartesian coordinates and energies of all the stationary points optimized in gas and implicit solvents. See DOI: 10.1039/b000000x/

- G. Sienel, R. Rieth and K. T. Rowbottom, *Ullmann's Encyclopedia of Organic Chemicals*, Wiley-VCH, Weinheim, **1999**.
- K. A. Joergensen, *Chem. Rev.* **1989**, *89*, 432..
- B. S. Lane and K. Burgess, *Chem. Rev.* **2003**, *103*, 2457.
- G. Grigoropoulou, J. H. Clark and J. A. Elings, *Green Chemistry* **2003**, *5*, 1.
- E. Collange, J. Garcia and R. Poli, *New J. Chem.* **2002**, *26*, 1249-1256.
- R. Poli, *Chem. Eur. J.* **2004**, *10*, 332-341.
- J.-E. Jee, A. Comas-Vives, C. Dinoi, G. Ujaque, R. V. Eldik, A. Lledos and R. Poli, *Inorg. Chem.* **2007**, *46*, 4103.
- A. Comas-Vives, A. Lledos and R. Poli, *Chem. Eur. J.* **2010**, *16*, 2147.
- A. M. Martins, C. C. Romao, M. Abrantes, M. C. Azevedo, J. Cui, A. R. Dias, M. T. Duarte, M. A. Lemos, T. Lourenço and R. Poli, *Organometallics* **2005**, *24*, 2582-2589.
- C. Dinoi, M. Ciclosi, E. Manoury, L. Maron, L. Perrin and R. Poli, *Chem. Eur. J.* **2010**, *16*, 9572-9584.
- See Supplementary Information for details in calculations.
- R. H. Holm, *Chem. Rev.* **1987**, *87*, 1401.
- J. P. Donahue, C. Lorber, E. Nordlander and R. H. Holm, *J. Am. Chem. Soc.* **1998**, *120*, 3259.
- G. C. Tucci, J. P. Donahue and R. H. Holm, *Inorg. Chem.* **1998**, *37*, 1602.
- H. Mimoun, I. Seree de Roch, L. Sajus, *Tetrahedron* **1970**, *26*, 37.
- I. V. Yudanov, *J. Struct. Chem.* **2007**, *48*, S111.
- I. V. Yudanov, P. Gisdakis, C. Di Valentin and N. Rosch, *Eur. J. Inorg. Chem.* **1999**, 2135.
- P. Gisdakis, S. Antonczak, S. Kostlmeier, W. A. Herrmann and N. Rosch, *Angew. Chem. Int. Ed. Engl.* **1998**, *37*, 2211.
- P. Gisdakis, I. V. Yudanov and N. Rosch, *Inorg. Chem.* **2001**, *40*, 3755.

